

See discussions, stats, and author profiles for this publication at: <https://www.researchgate.net/publication/332443480>

Time-Resolved Directional Brain-Heart Interplay Measurement Through Synthetic Data Generation Models

Article in *Annals of Biomedical Engineering* · April 2019

DOI: 10.1007/s10439-019-02251-y

CITATIONS

50

5 authors, including:



Vincenzo Catrambone

Università di Pisa

87 PUBLICATIONS 576 CITATIONS

SEE PROFILE



Nicola Vanello

Università di Pisa

147 PUBLICATIONS 2,156 CITATIONS

SEE PROFILE

READS

161



Alberto Greco

Università di Pisa

156 PUBLICATIONS 2,844 CITATIONS

SEE PROFILE



Enzo Pasquale Scilingo

Università di Pisa

359 PUBLICATIONS 8,778 CITATIONS

SEE PROFILE

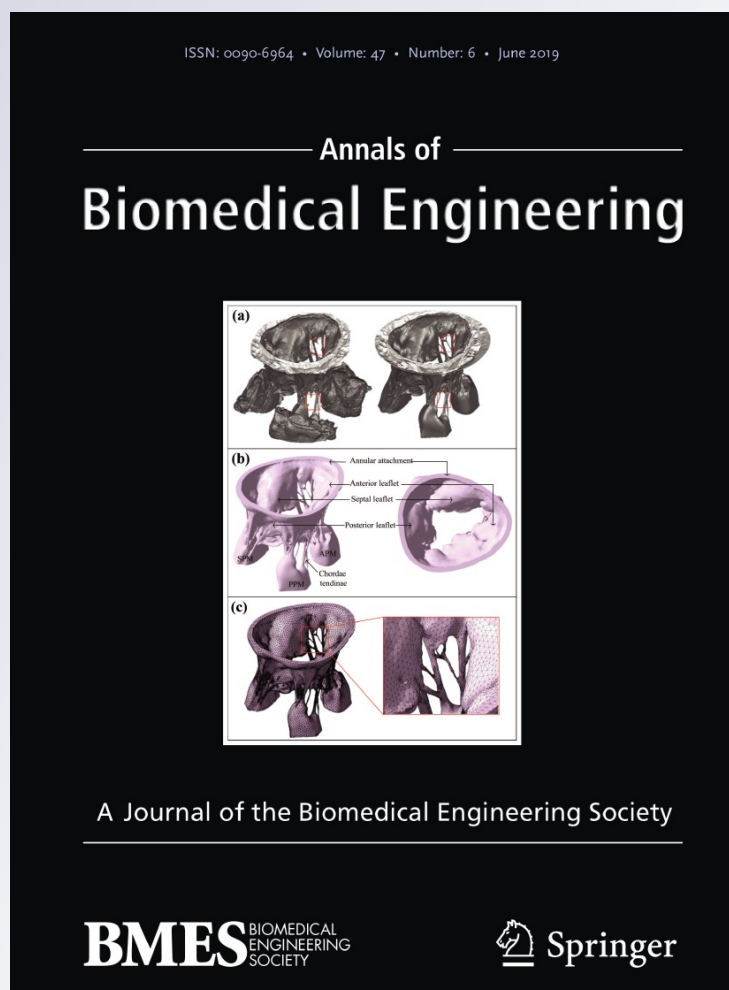
Time-Resolved Directional Brain–Heart Interplay Measurement Through Synthetic Data Generation Models

**Vincenzo Catrambone, Alberto Greco,
Nicola Vanello, Enzo Pasquale Scilingo
& Gaetano Valenza**

Annals of Biomedical Engineering
The Journal of the Biomedical
Engineering Society

ISSN 0090-6964
Volume 47
Number 6


Ann Biomed Eng (2019) 47:1479–1489
DOI 10.1007/s10439-019-02251-y



Your article is protected by copyright and all rights are held exclusively by Biomedical Engineering Society. This e-offprint is for personal use only and shall not be self-archived in electronic repositories. If you wish to self-archive your article, please use the accepted manuscript version for posting on your own website. You may further deposit the accepted manuscript version in any repository, provided it is only made publicly available 12 months after official publication or later and provided acknowledgement is given to the original source of publication and a link is inserted to the published article on Springer's website. The link must be accompanied by the following text: "The final publication is available at link.springer.com".



Time-Resolved Directional Brain–Heart Interplay Measurement Through Synthetic Data Generation Models

VINCENZO CATRAMBONE , ALBERTO GRECO, NICOLA VANELLO, ENZO PASQUALE SCILINGO,
and GAETANO VALENZA

Bioengineering and Robotics Research Center E.Piaggio & Department of Information Engineering, School of Engineering,
University of Pisa, Largo Lucio Lazzarino 1, 56122 Pisa, Italy

(Received 27 November 2018; accepted 21 March 2019; published online 15 April 2019)

Associate Editor Joel Stitzel oversaw the review of this article.

Abstract—Although a plethora of synthetic data generation models have been proposed to validate biomarkers of brain and cardiovascular dynamics separately, a limited number of computational methods estimating directed brain–heart information flow are currently available in the scientific literature. This study introduces a computational framework exploiting existing generative models for a novel time-resolved quantification of causal brain–heart interplay. Exemplarily, having electroencephalographic signals and heart rate variability series as inputs, respective synthetic data models are coupled through parametrised functions defined in accordance with current central autonomic network (CAN) knowledge. We validate this concept using data from 30 healthy volunteers undergoing notable sympathetic elicitation through a cold-pressor test, and further compare the obtained results with a state-of-the-art method as maximal information coefficient. Although our findings are in agreement with previous CAN findings, we report new insights into the role of fronto-parietal region activity and lateralisation mechanisms over the temporal cortices during prolonged peripheral elicitation, which occur with specific time delays. Additionally, the afferent autonomic outflow maps to brain oscillations in the δ and γ bands, whereas complementary cortical dynamics in the θ , α , and β bands act on efferent autonomic control. The proposed framework paves the way towards novel biomarker definitions for the assessment of complex physiological networks using existing data generation models for brain and peripheral dynamics.

Keywords—Heart rate variability, Electroencephalography, Central autonomic network, Brain–heart interplay.

INTRODUCTION

The quantitative assessment of physiological systems interplay is fundamental for understanding biological functions in health and disease. Because of these interactions, physiological networks demonstrate properties that the individual sub-systems acting alone cannot.²

A paradigmatic example refers to the central nervous system (CNS) and autonomic nervous system (ANS) interplay. These systems concurrently regulate all peripheral organs through anatomical, biochemical, and other functional (e.g., hormonal, vascular) links, influencing each other continuously.

The existence of a central autonomic network (CAN)⁴ and its influence on the cardiovascular system through the brainstem has been proposed associating the control of the activity of parasympathetic and sympathetic preganglionic neurons with a distributed area of the neuraxis (i.e. CAN).^{3,4} The left amygdala, mid-cingulate cortex and left posterior and right anterior insular cortices constitute the core of CAN brain areas.³ Furthermore, along with brainstem areas, the hypothalamus generates autonomic patterns that regulate peripheral homeostasis. Anterior limbic paths are linked to emotional and behavioural processing.⁴

These findings are directly related to clinical evidence. Cerebrovascular accidents and transient ischaemic attacks (transient episodes of neurological dysfunction caused by the loss of blood flow) are frequently caused by cardiac arrhythmias,¹⁸ and atrial fibrillation may also result in cognitive disorders.^{9,12} Additionally, brain disorders, including stroke and epilepsy, are considered to occur secondary to envi-

Address correspondence to Vincenzo Catrambone, Bioengineering and Robotics Research Center E.Piaggio & Department of Information Engineering, School of Engineering, University of Pisa, Largo Lucio Lazzarino 1, 56122 Pisa, Italy. Electronic mail: vincenzo.catrambone@ing.unipi.it

ronmental stress (e.g., panic disorders and emotional distress) and may lead to cardiovascular disorders.^{10,26}

Despite the aforementioned evidence, the brain and heart have long been studied separately through *ad hoc* techniques and methodologies characterising specific single-system dynamics at the cortical/sub-cortical or peripheral level.²⁷ In fact, in a given experimental set-up, although data acquisition of brain and cardiac dynamics is often concurrently performed, data processing is usually treated separately (e.g., spectral analysis is performed over electroencephalographic (EEG) signals on the brain side, and over heart rate variability (HRV) series on the heart side), therefore neglecting most of the multivariate, complex information underlying brain–heart interplay.^{3,25,27}

At the methodological level, a few recent studies have attempted to mathematically couple brain data in conjunction with peripheral signals related to ANS activity.^{2,11,13,20,22,23,31} Exemplarily, among a variety of coupling functions suitable for this aim, (review in Ref. 22) measures of Granger causality (GC), maximum information coefficient (MIC), and multivariate linear models have been exploited.^{2,11,13} GC quantifies the causal information flow between variables by inferring how much brain activity can be explained in isolation or by the knowledge of heartbeat dynamics¹¹ and *vice versa*. Time-delay stability² is linked to the maximum cross-correlation function between the two systems, whereas MIC quantifies linear and nonlinear coupling between concurrent brain–heart outflows.³⁰ Other studies have focused on improving time-delay stability performance,¹³ correlating CAN activity and heartbeat-derived series,^{28,29} cross-frequency coupling²³ and high-resolution joint symbolic analysis.²⁰ Although these studies demonstrated the feasibility and high impact of combined brain–heart interplay assessment, a physiologically inspired multivariate modelling framework allowing for an *ad hoc*, fully parametric estimation of brain–heart interplay is missing. In fact, GC was not specifically devised for the assessment of brain–heart interactions and has been recently criticised,²⁴ while MIC, time-delay stability, and other multivariate methods do not account for directionality estimation.

To this aim, we propose a novel computational framework in the field of brain–heart interplay, exploiting synthetic data generation models. We prove the concept by demonstrating how to simply not trivially quantify the time-varying interplay occurring from-heart-to-brain, as well as from-brain-to-heart. Previously validated physiologically inspired models of cortical activity, as well as heartbeat generation models, are coupled in accordance with state-of-the-art CAN knowledge. Then, multisystem coupling measures, namely, from-heart-to-brain $C_{Heart \rightarrow Brain}(t)$ and

from-brain-to-heart $C_{Brain \rightarrow Heart}(t)$ coefficients, can be derived by solving the inverse problem.

We devise a new model of brain–heart interplay considering EEG and HRV series as inputs and brain–heart interplay measurements as outputs. Such measurements can be derived in a time-resolved, directional fashion to account for the non-stationarity of brain–heart interactions. The results are gathered from 30 healthy volunteers undergoing prolonged sympathetic elicitation through a cold-pressor (CP) test, which is known to indirectly activate the baroreflex and has been extensively employed for the study of psychosomatic illnesses, the autonomic response to stress, psychological disorders, autonomic responsiveness and more generally, cortical influences on autonomic functions.⁷ Result from the proposed model are then compared with the ones from a MIC analysis. A preliminary version of this work has been reported in Ref. 6.

MATERIALS AND METHODS

We describe the concept of novel metric derivation by coupling formulations of EEG and heartbeat generative mechanisms based on adaptive Markov process amplitude (AMPA)¹ and integral pulse frequency modulation (IPFM),⁵ respectively. We then formalise how to properly couple these models and solve the associated inverse problem to adaptively estimate the new brain–heart directional coupling coefficients. Furthermore, we briefly describe the MIC computation that will be taken as a reference state-of-the-art coupling estimation.

Adaptive Markov Processes for EEG Signal Generation

EEG modelling based on AMPA is a computationally effective method that links dynamic-specific frequency bands. The model accounts for a linear combination of K oscillators whose main frequency corresponds to the classical electro-physiological set $B \in \{\delta, \theta, \alpha, \beta, \gamma\}$. The amplitudes of the oscillations are defined by the following stochastic Markov process:

$$\begin{aligned} \text{EEG}(t_n) &= \sum_{j=1}^K a_j(t_n) \sin(\omega_j t_n + \phi_j) \\ a_j(t_n) &= \eta_j a_j(t_{n-1}) + \xi_j(t_{n-1}) \end{aligned} \quad (1)$$

where t_n is the n -th time sample, ϕ_j and η_j are constants, ω_j is the main frequency associated with the EEG bandwidths B and corresponding pulsation $\omega_j|_{\{f_j = \max_{[B_{\min}, B_{\max}]} B\}} = 2\pi f_j$ at central frequency f , $\xi_j =$

$\mathcal{N}(0, \sigma_j)$ is a Gaussian white noise source with standard deviation σ_j , where $\xi_j(t_n)$ is defined as independent from $\xi_i(t_m)$, for any given m and i . The EEG signal is modelled as the sum of 5 oscillations, whose main frequency refers to the classical EEG bands. Amplitude of these oscillations are time-varying, whose history dependence follows a first-order Markov chain with white noise. This formulation accounts for the intrinsic non-stationarity of physiological dynamics, and uses empirical parameter set to generate synthetic EEG signals. Further details are provided in Ref. 1.

Integral Pulse Frequency Modulation for Heartbeat Generation

We consider an IPFM model to describe heartbeat dynamics in a parametric fashion.⁵ In particular, a beat-to-beat integral is defined over the summation of two oscillators mimicking the sympathetic-parasympathetic autonomic outflow, whose amplitudes are given by the constant terms C_s and C_p . In detail:

$$RR(t) = \sum_{k=1}^N \delta'(t - t_k) \quad (2)$$

where δ' is the Dirac delta function, t is the continuous time, and t_k is the time of the k -th heartbeat occurrence depending on:

$$1 = \int_{t_k}^{t_{k+1}} [HR + m(t)] dt \quad (3)$$

with HR , the mean heart rate expressed in Hz, and $m(t)$, the input autonomic activity:

$$m(t) = C_s \sin(\omega_s t) + C_p \sin(\omega_p t) \quad (4)$$

with C_s and C_p as the sympathetic and parasympathetic coupling constants, respectively, and ω_s and ω_p as the related pulsations. Intuitively, the IPFM model describes how heartbeat events are modulated by autonomic activity, which is represented by the input signal $m(t)$. Once the integral function reaches a threshold (set to 1) the pulse is generated and the integrator is reset to 0. In this way, the IPFM model generates cardiac events at a mean frequency fixed to HR if the modulation function is null. Further details are provided in Ref. 5.

The Proposed Brain-Heart Modelling Framework

The EEG and heartbeat generation models are merged into a multivariate framework aiming to exploit the coupling measures that can be derived therein.

Formally, the Markovian brain activity generation also uses heartbeat dynamics as an input through the Ψ_j function, defining the coupling from-heart-to-brain:

$$EEG(t_n) = \sum_{j=1}^K a_j(t_n) \sin(\omega_j t_n + \phi_j) \quad (5)$$

$$a_j(t_n) = \eta_j a_j(t_{n-1}) + \xi'_j(t_{n-1}) + \Psi_j(t_{n-1} | P_{B_C}(t_{n-1}), C_{B_C \rightarrow j}(t_{n-1})) \quad (6)$$

where $j \equiv B$, $B_C \in \{LF = [0.04, 0.15]Hz, HF = [0.15, 0.4]Hz\}$, and $C_{B_C \rightarrow j} \equiv C_{Heart \rightarrow Brain}$. As a first attempt, we apply the following simple not-trivial relationship:

$$\Psi_j(t_{n-1}) = C_{B_C \rightarrow j}(t_{n-1}) \times P_{B_C}(t_{n-1} | \mathcal{H}_t^C) \quad (7)$$

with heartbeat history \mathcal{H}_t^C and:

$$P_{B_C}(t_{n-1}) = \int_{B_C} \int_{T_C} PSD_{RR}(f, t) dt df \quad (8)$$

for $T_C \in (t - W_{RR}, t_{n-1}]$, W_{RR} is the time window on the RR intervals, and $PSD_{RR}(f, t)$ is the related time-frequency representation, which is calculated using the smoothed pseudo-Wigner-Ville distribution method (SPWVD),¹⁵ whose formulation is given in Eq. (9),

$$PSD_{RR}(f, t) = \int_{-\infty}^{\infty} \phi_d(\tau) \times \left[\int_{-\infty}^{\infty} \phi_t(t - v) x(v - \frac{\tau}{2}) x^*(v - \frac{\tau}{2}) dv \right] e^{-j2\pi f \tau} d\tau, \quad (9)$$

where: ϕ_d and ϕ_t are smoothing functions (the first an exponential window and the latter a rectangular window), and $x(t)$ the RR interval series. The SPWVD application is justified by the resulting time-frequency resolution with respect to a non-parametric formulation, which is associated with low variance of the estimated power and independent control of time and frequency filtering.¹⁷

Formally:

$$m(t_n) = C_{LF}(t_n) \sin(\omega_{LF} t_n) + C_{HF}(t_n) \sin(\omega_{HF} t_n) \quad (10)$$

$$C_{LF}(t_n) = C'_s + \Psi_{LF}(t_{n-1} | P_j(t_{n-1}), C_{j \rightarrow LF}(t_{n-1})) \quad (11)$$

$$C_{HF}(t_n) = C'_p + \Psi_{HF}(t_{n-1} | P_j(t_{n-1}), C_{j \rightarrow HF}(t_{n-1})) \quad (12)$$

with $C_{j \rightarrow B_C} \equiv C_{Brain \rightarrow Heart}$.

In this study, we propose the following proportional coupling function $\Psi_{B_C}(t_{n-1})$:

$$\Psi_{B_C}(t_{n-1}) = C_{j \rightarrow B_C}(t_{n-1}) \times P_j(t_{n-1} | \mathcal{H}_t^B) \quad (13)$$

where $B_C \in \{HF, LF\}$ as in Eqs. (11) and (12), and \mathcal{H}_m^B is the brain activity history:

$$P_j(t_{n-1}) = \int_j \int_{T_E} PSD_{EEG}(f, t) dt df \quad (14)$$

for $T_E \in (t - W_{EEG}, t_{n-1}]$, with W_{EEG} as the time window on the EEG series and $PSD_{EEG}(f, t)$ as the related time-frequency representation, obtained through the well-known short time Fourier transform as a standard estimation method:

$$PSD_{EEG}(f, t) = \int_{-\infty}^{\infty} x(\tau) w(t - \tau) e^{-j2\pi f\tau} d\tau \quad (15)$$

where $w(t)$ is a time-shifted window, and $x(t)$ is the EEG signal.

In Eqs. (7) and (13), the time-resolved directional metrics of interest are: $c_{B_C \rightarrow j}(t)$, $c_{j \rightarrow B_C}(t)$, respectively. These metrics represent the instantaneous interplay between the brain and heart in the two outflow directions, whose magnitude changes are reasonably linked to relevant physiological or pathological conditions. The rationale underlying this formulation is that the activity of one interacting system (e.g., sympathetic arousal for cardiovascular dynamics) is modulated by activity of the other system (e.g., α power desynchronisation for brain dynamics). Exemplarily, a positive value indicates a proportional functional correlation between systems, i.e., the processes underlying an increased EEG power spectrum are also linked to increased vagal and/or sympatho-vagal outflow through RR interval modulation. A (close to) zero value is associated with no relevant interactions between the two systems.

Derivation of New Directional Brain–Heart Coupling Measures

Aiming to derive novel brain–heart coupling measures, we report the inverse model formulation considering EEG and HRV series as inputs.

Regarding $C_{Brain \rightarrow Heart}(t)$, the following estimates apply: HR is derived as the inverse of the average between all RR intervals occurring in T_E , whereas C_{LF} and C_{HF} are calculated as in Eq. (16).⁵

$$\begin{aligned} \begin{bmatrix} C_{LF}(t_n) \\ C_{HF}(t_n) \end{bmatrix} &= \frac{1}{\sin(\omega_{HF}/2HR) - \sin(\omega_{LF}/2HR)} \\ &\times \begin{bmatrix} \frac{\sin(\omega_{HF}/2HR)\omega_{LF}HR}{4\sin(\omega_{LF}/2HR)} & \frac{-\sqrt{2}\omega_{LF}HR}{8\sin(\omega_{LF}/2HR)} \\ \frac{-\sin(\omega_{LF}/2HR)\omega_{HF}HR}{4\sin(\omega_{HF}/2HR)} & \frac{\sqrt{2}\omega_{HF}HR}{8\sin(\omega_{HF}/2HR)} \end{bmatrix} \begin{bmatrix} L_1 \\ L_2 \end{bmatrix} \end{aligned} \quad (16)$$

In Eq. (16) L_1 and L_2 are estimated as key features of the RR Poincaré plot: L_1 is the RR range (considering the difference between the maximum and minimum RR interval time lengths) within T_E , whereas $L_2 = \sqrt{2} \max_k (RR_k - RR_{k-1})$.

$$C_{j \rightarrow B_C}(t_n) = \frac{(C_{B_C}(t_n) - C_s)}{P_j(t_n)} \quad (17)$$

The $C_{Heart \rightarrow Brain}(t_n)$ is estimated through the well known least square procedures, considering that Eq. (5) is an autoregressive model with exogenous inputs.

Formally, given $\Xi = A - \Psi\Theta$, with the variables defined in Eq. (18), the obtained result is: $\Theta = (\Psi'\Psi)^{-1}\Psi'A$.

$$\begin{aligned} \Xi &= [\xi_{B_E}(t_n) \dots \xi_{B_E}(t_n - m + 1)]; \\ A &= [a_{B_E}(t_n) \dots a_{B_E}(t_n - m + 1)] \\ \Psi &= \begin{bmatrix} a_{B_E}(t_n - 1) & P_{B_C}(t_n - 1) \\ \vdots & \vdots \\ a_{B_E}(t_n - m) & P_{B_C}(t_n - m) \end{bmatrix} \\ \Theta &= \begin{bmatrix} \eta_{B_E} & \dots & \eta_{B_E} \\ C_{B_C \rightarrow B_E}(t_n - 1) & \dots & C_{B_C \rightarrow B_E}(t_n - m) \end{bmatrix} \end{aligned} \quad (18)$$

Maximum Information Coefficient

Maximum information coefficient (MIC)¹⁹ is a metrics quantifying a linear or nonlinear coupling between two data vectors. Starting from a scatterplot of the ordered pairs of two vectors, x and y , it is possible to determine a number of rows and columns resulting in different space partitions. By indicating the sample of all the possible partitions with $G_{x \times y}$, and the mutual information of a specific partition with I_g , it is possible to define $m_{x \times y}$ as follows:

$$m_{x \times y} = \frac{\max\{I_g\}}{\log \min\{x, y\}} \quad (19)$$

where n is the dimension of the vectors. MIC is derived as the maximum over $m_{x \times y}$ of all the ordered pairs (x, y) ; formally, it is possible to estimate $MIC = \max_{xy < B} \{m_{x \times y}\}$ with B empirically defined as $B = n^{0.6}$. Further detail are reported in Ref. 19.

Experimental Setup and Signal Pre-processing

A total of 30 right-handed healthy volunteers (15 males, 15 females; 26.7 years on average) provided

informed consent to participate to the study. Subjects had no history of neurological, cardiovascular, or respiratory disease. Data from three subjects were discarded due to artefacts. Participants were asked to fulfil behavioural and cognitive tests before and after the following tasks: 3-min resting state; up to 3-min CP test.

Throughout the protocol, subjects were asked to keep closed eyes to minimise artefacts while multivariate physiological signals including one-lead ECG and high-density 128-channel EEG were recorded (analogue-to-digital converter resolution of 24 bit). The reference EEG channel map is reported in the Supplementary Information. Participants were asked to sit comfortably on a chair before data recording to ensure a hemodynamic stabilisation. For the CP test, subjects were guided in submerging their left (i.e., non-dominant) hand, up to wrist, into a bucket filled with ice and water (between 0 and 4 °C) for up to 3 min, consistent with the average pain threshold of healthy people.⁸ In the case of early pain, subjects were free to remove their hand from the ice bucket and move to the next session. All experimental procedures were approved by the local ethical committee Area Vasta Nord-Ovest Toscana.

EEG and ECG-HRV pre-processing steps are extensively detailed in Ref. 30. Briefly, EEG pre-processing comprised bad channel rejection using principal component analysis, re-referencing the all-channel average; bandpass filtering between 0.5 Hz and 45 Hz using a 10th order Butterworth filter; ICA decomposition to remove eye blink, ECG, electromyogram, head movements and other artefact sources; and visual data inspection. On the heart side, R-peaks were identified from ECG through the well-known Pan-Tompkins algorithm to obtain the RR interval series. Physiological and algorithmic artefacts were corrected through local log-likelihood point-process statistics devised for cardiac dynamics (see Ref. 30 and references therein).

RESULTS

We report experimental results gathered from synthetic and actual brain-heart data. The former aims to validate the estimation formulation through the in-

verse model solutions, which is then applied to real data gathered from healthy subjects undergoing resting state, CP test. These results on CP test from the proposed model are then compared with the one from a MIC analysis. Throughout this section, the following ranges are fixed: from the heart side, $B_C \equiv \{LF = [0.04, 0.15]; HF = [0.15, 0.4]\}$, and from the brain-side $j \in \{\delta = [0.5, 4], \theta = [4, 8], \alpha = [8, 12], \beta = [12, 30], \gamma = [30, 45]\}$, all expressed in Hz. The P_j was estimated through a standard short-time Fourier transform with a Hanning window of 1 s length and 1 s step size, whereas P_{B_C} was derived using a smoothed pseudo-Wigner-Ville distribution method (details in Ref. 15) with the following parametric values: $W_{RR} = W_{EEG} = 15$ s; $\omega_{LF} = 2\pi 0.01$ rad/s, $\omega_{HF} = 2\pi 0.25$ rad/s.

Synthetic Data

By implementing the model reported in “[The Proposed Brain-Heart Modelling Framework](#)”, we generated seven sets of synthetic brain-heart data with noise $\sigma'_\theta = \{0.5, 1, 1.5, 2, 2.5, 3, 6\}$ related to $\xi'_\theta(t_{n-1}) = \mathcal{N}(0, \sigma'_\theta)$. A total of 50 multivariate synthetic series were generated for each of the seven noise levels. Throughout the simulation, time-varying coefficients $C_{BC \rightarrow j}$ and $C_{j \rightarrow BC}$ were superimposed, and their values ranged from 0 to 1, with a step of 0.1. Other set parameters are reported in Table 1. The results shown in Fig. 1, highest row, consider a brain-heart coupling superimposed between the EEG θ band and HRV-HF power.

The results show that the proposed estimation can follow the superimposed, directional brain-heart couplings despite the noise level.

Cold-Pressor Test

Coupling coefficients $C_{j \rightarrow BC} \equiv C_{Brain \rightarrow Heart}$ and $C_{BC \rightarrow j} \equiv C_{Heart \rightarrow Brain}$ were estimated from real brain-heart data during CP elicitation and resting phase (see details in “[Experimental Setup and Signal Pre-pro-](#)

TABLE 1. Synthetic data model parameters.

	Short description	Values
HR	HRV constant term	1.18
ω_S	Sympathetic main freq. (Hz)	$2\pi \times 0.1$
ω_P	Parasympathetic main freq. (Hz)	$2\pi \times 0.25$
C_S	Sympathetic constant term	0.25
C_P	Parasympathetic constant term	0.24
ω_k	EEG main frequencies (Hz)	[1.27; 5.66; 9.44; 20.8; 34.1]
σ_k	Std.Dev. white noises	[1; σ'_θ ; 1.81; 2.02; 2.07]
γ_k	EEG constant terms	[0.76; 0.86; 0.87; 0.86; 0.83]
F_s	Sampling frequency (Hz)	256

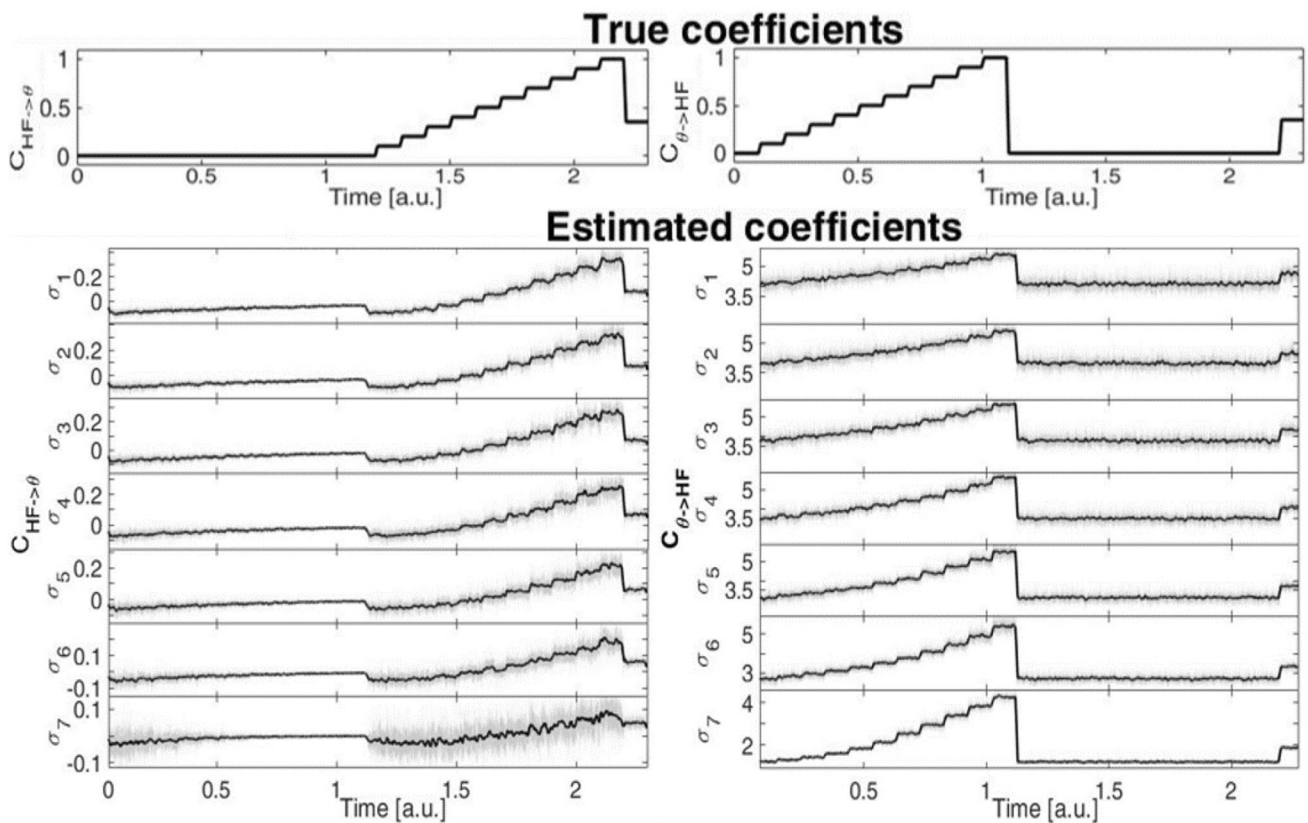


FIGURE 1. The superimposed coupling coefficients are shown in the top row, whereas the estimated ones follow below. The second to the eighth rows show estimates with the standard deviation of noise as 0.5, 1, 1.5, 2, 2.5, 3, and 6 respectively. The black line indicates the median value among 50 series, while the grey area indicates the median absolute deviation across the series.

cessing”). Group-wise median values for all coefficients (from-brain-to-heart and vice versa) can be found in the Supplementary Information.

Figures 2 and 3 show p -value topographic maps resulting from the statistical comparison (non-parametric Wilcoxon test for paired data) of $C_{j \rightarrow B_C}$ and $C_{B_C \rightarrow j}$ between resting state and CP sessions, considering both HRV-HF and HRV-LF power, and the five EEG frequency bands. The significance level was adjusted for multiple comparisons in accordance with a permutation test. In this first step, for each subject the time-varying brain–heart information was condensed through the median values calculated within the last 3 min of rest and the 3 min of CP.

The results in Fig. 2 highlight a significant decrease in the directional coupling from the afferent vagal system to the brain structure linked to δ and γ cortical oscillations induced by CP elicitation. In particular, $C_{HF \rightarrow \delta}$ decreases over the midline central-frontal region, in the bilateral somatosensory areas, and in the contralateral temporal region, whereas $C_{HF \rightarrow \gamma}$ decreases in the central-frontal region and ipsilateral prefrontal area. Similar dynamics have been found in the directional coupling from the

afferent sympatho-vagal system to the brain (see the top row of Fig. 3).

Conversely, the directional coupling from-brain-to-vagal system significantly increased during the prolonged baroreflex elicitation, mainly involving cortical oscillations over the ipsilateral frontal and prefrontal lobes for cortical oscillations in the θ and α bands and over the midline cortices for oscillations in the β band. A generally decreasing coupling during CP with respect to the resting state can be observed for the information outflow going from the brain to the sympatho-vagal system, as clearly shown in Fig. 3. In this case, oscillations in the θ band mainly involve the contralateral somatosensory and occipital regions and the ipsilateral region in the γ band. Importantly, these results suggest lateralisation mechanisms occurring between ANS and tonic cortical activity in the θ band. In fact, within this frequency band, control of the heart by the brain occurs through the left fronto-temporal-occipital areas, whereas the projection of heartbeat dynamics onto the brain seems to be mapped over the right frontal and temporal regions.

Further considerations can be drawn by analysing the group-wise, time-varying dynamics of the proposed

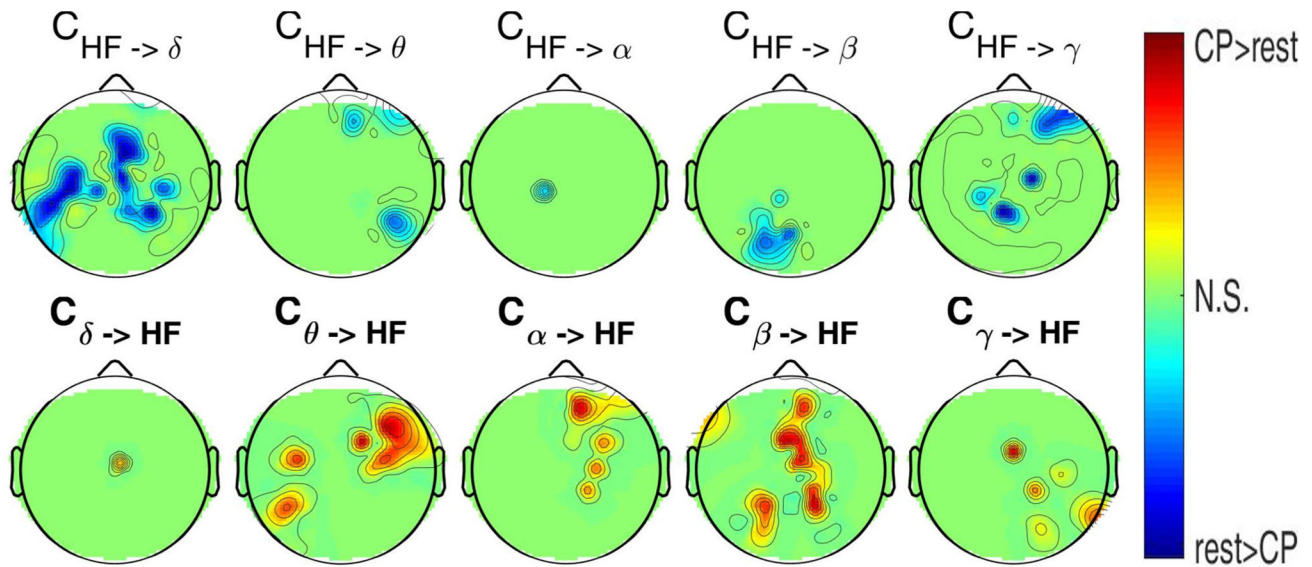


FIGURE 2. p -value topographic maps from non-parametric Wilcoxon tests for directional brain-heart (HRV-HF band) between resting state and CP elicitation. The top row shows results from from-heart-to-brain coupling analysis, whereas the bottom row shows from-brain-to-heart ones. Green areas indicate no significant differences in coupling between sessions, whereas red (blue) areas indicate significant differences between sessions with a higher (lower) brain-heart coupling associated with the CP phase.

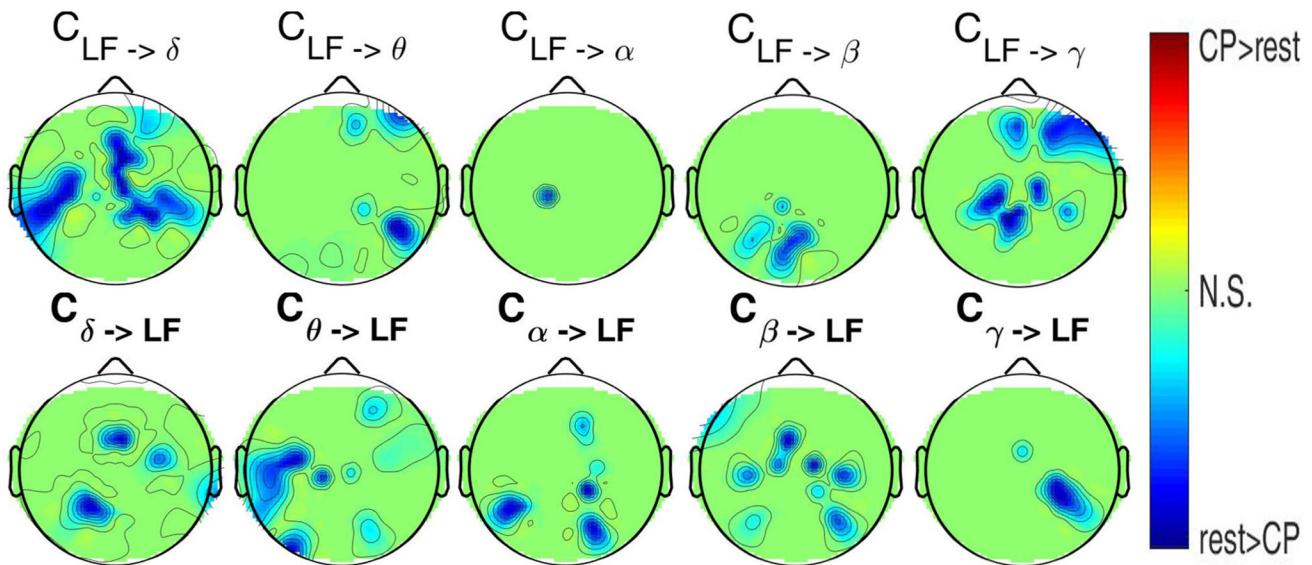


FIGURE 3. p -value topographic maps from non-parametric Wilcoxon tests for directional brain-heart (HRV-LF band) between resting state and CP elicitation. The top row shows results from from-heart-to-brain coupling analysis, whereas the bottom row shows from-brain-to-heart ones. Green areas indicate no significant differences in coupling between sessions, whereas red (blue) areas indicate significant differences between sessions with a higher (lower) brain-heart coupling associated with the CP phase.

brain-heart interplay indices. Figures 5, 6 show exemplary temporal dynamics from statistically significant EEG series placed over physiologically relevant areas and specific frequency bands. Notably, a significant decrease from-heart-to-brain occurs approximately 60 s after the CP elicitation for both LF and HF spectra, reaching the minimum in approximately 90 s. Alternatively, the interplay going from-

brain-to-heart changes sooner in an opposite manner between the LF and HF. Specifically, a significant increase in the coupling from the brain to the vagal system occurred approximately 30 s after the CP initiation, while the exemplary $C_{\gamma \rightarrow LF}$ dynamics showed a quick decrease in coupling immediately after the beginning of the insertion of the hand into the ice water (Fig. 6).

MIC Analysis

Figure 4 shows p -value topographic maps resulting from the statistical comparison (non-parametric Wilcoxon test for paired data) of MIC values between resting state and CP test sessions, over all frequency bands. Results indicate that combined brain–heart oscillations γ – LF and γ – HF have a higher MIC during resting phase than CP, particularly over the central parietal (for γ – LF) and central pre-frontal (in both γ – LF and γ – HF) areas. For the other oscillations, brain–heart coupling increases during CP test with the exception of θ – HF oscillations. Central–parietal areas show to be consistently different among different frequencies. The same applies for the pre-frontal right (contralateral) regions. Vagal oscillations seem to preferentially interact with brain oscillations in the θ , α , β bands over the pre-frontal and temporal (somatosensory areas) regions.

A region-wise comparison between a MIC analysis and the proposed brain–heart model is reported in the Supplementary Information. At a qualitative level, brain areas identified by a MIC analysis maybe considered as a subset of the regions highlighted by the proposed model, which also enriches the results with directionality information while uncovering more brain regions that are with lower p -values than MIC .

DISCUSSION

This study presents a novel, fully parametric modelling framework to dynamically estimate the directional interactions occurring between brain and

cardiovascular dynamics by exploiting existing generative models of synthetic data. Interplay estimates are derived from *ad hoc* equations of multivariate physiological dynamics rather than being adapted from existing signal processing frameworks (e.g., MIC , GC , or similar approaches).

In particular, we propose to exploit equations that have been previously validated for physiological simulation purposes to define new biomarkers derived from coupling functions, which are formalised in accordance with the current CAN knowledge. Given the substantial number of synthetic generative models that have been proposed in the scientific literature, the proposed approach allows for potentially defining a high number of biomarkers for multisystem modelling.

Here, we prove the concept exploiting previously validated EEG and RR interval series generation models to study effective brain–heart interactions. These models were properly coupled to devise new markers of such a directional information outflow, which are directly derived by solving the inverse problem. We validate the framework using both synthetic and real data. The synthetic data results prove the reliability of our estimation at different noise levels. Experimental data were gathered from healthy volunteers undergoing sympatho-vagal perturbations through a CP test. Notably, CP has been extensively used to study cortical influences on autonomic functions and *vice versa*.^{7,14,21}

Results from the proposed model are consistent with the one from a MIC analysis, therefore supporting their reliability. Indeed, the methods show overlapping brain regions whose activity is significantly

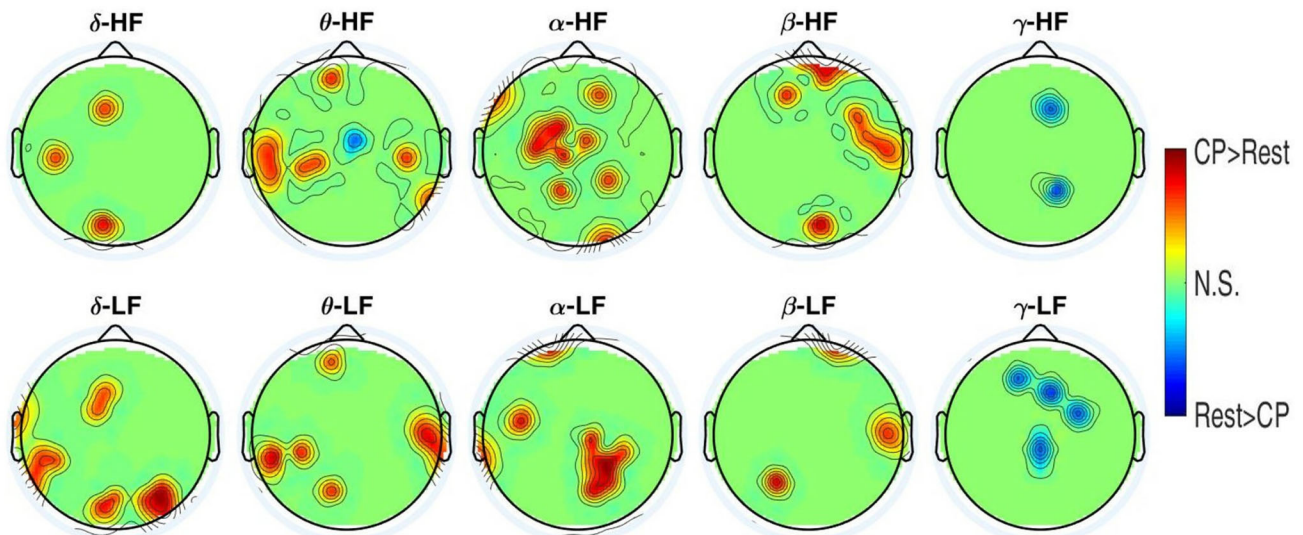


FIGURE 4. p -value topographic maps from non-parametric Wilcoxon tests, for the MIC analysis, between resting state and CP test sessions. Green areas indicate not significant changes between sessions.

altered by the CP test, with respect to a resting state (see details in the Supplementary Information). Note, however, that MIC is an always positive metrics, and does not provide information on the directionality of the coupling.

Our results are consistent with previous evidence showing delayed cardiac autonomic responses between 26 and 57 s during CP,¹⁶ allowing us to make the following speculative claim. Following strong sympatho-vagal changes due to prolonged baroreflex elicitation, enhanced brain activity directed towards cardiovascular control occurs first, and after approximately 25 s (i.e., 1/0.04 Hz), the autonomic outflow on the sinoatrial node starts to significantly change heartbeat dynamics. Then, after approximately 50–60 s, the cardiac autonomic outflow starts increasing the information exchange towards specific CAN areas.

In general, our results highlight a faster dynamical interaction between the brain and parasympathetic tone than the sympathetic ones (see Figs. 5 and 6).

Limitations of this study are mainly related to the specific models used for EEG and heartbeat data generation, the choice of specific parameter values, and the absence of gold-standard experimental tests to selectively activate directional brain–heart coupling. Indeed, the AMPA model does not account for the linear and nonlinear interactions between brain oscillations occurring at different frequency. Future works will be directed towards the implementation of such interaction effects into the proposed brain–heart model. However, the framework is empirically validated by obtaining physiologically plausible synthetic

EEG and RR intervals from the coupled model in Eqs. (5) and (12) (data not shown), and is flexible enough to translate the methodological foundations to other models, including fMRI/MEG/fNIRS generation as well as other autonomic covariates (e.g., respiration and blood pressure). The presented work proposes a new framework in the field of brain–heart interplay, defining a joint generative model that accounts for the mutual brain and heart activities. The proposed framework exploits a physiologically-inspired model concerning the definition of heartbeat dynamics, while embeds a data-driven model for EEG generation.

Our proposal represents a first attempt to address the brain–heart interplay modelling, quantifying mainly functional links between brain and heartbeat dynamics. Future developments will be focused on defining a more detailed, physiologically-inspired dynamics. Particularly, at the moment the proposed framework does not account for interplays between different power bands of the same signal (e.g. HF and LF, or α and β) which are known to be related to brain and heartbeat nonlinear dynamics.

Future endeavours will also focus on the investigation of directional brain–heart coupling in several physiological and pathological conditions, considering heartbeat oscillations in the LF and HF bands while estimating ω_{LF} and ω_{HF} from experimental data. Additionally, the study of model-derived synthetic data, gender differences, and time-varying p -value topographic maps will be pursued.

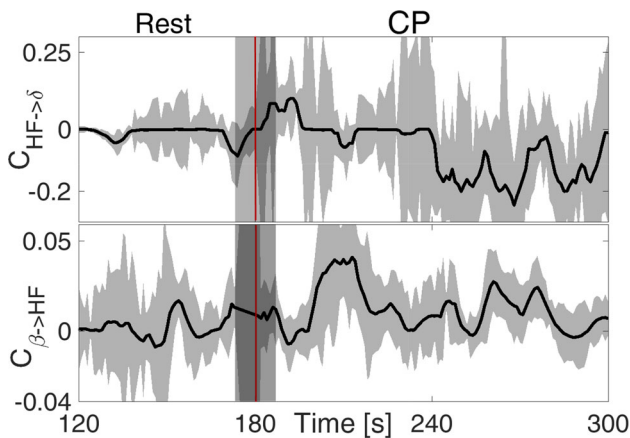


FIGURE 5. Exemplary time-varying $C_{\text{Heart} \rightarrow \text{Brain}}$ and $C_{\text{Brain} \rightarrow \text{Heart}}$ statistics computed from rest-CP heartbeat data among 27 subjects (from channel 35 of the EGI net, in the left fronto-temporal region). From the central region, the estimated $C_{HF \rightarrow \gamma}$ and $C_{\beta \rightarrow HF}$ are shown as the median (continuous black line) and $1.4826MAD(X)/\sqrt{n}$ (grey area). The vertical red line and superimposed grey area indicate the transition between the resting state and CP.

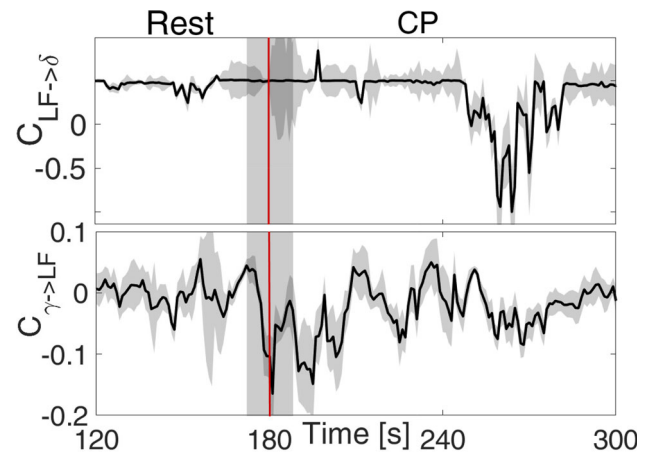


FIGURE 6. Exemplary time-varying $C_{\text{Heart} \rightarrow \text{Brain}}$ and $C_{\text{Brain} \rightarrow \text{Heart}}$ statistics computed from rest-CP heartbeat data among 27 subjects (from channel 6 of the EGI net, in the central-frontal brain area). From the central region, the estimated $C_{LF \rightarrow \delta}$ and $C_{\gamma \rightarrow LF}$ are shown as the median (continuous black line) and $1.4826MAD(X)/\sqrt{n}$ (grey area). The vertical red line and superimposed grey area indicate the transition between the resting state and CP.

Conclusion

In conclusion, our results show a new characterisation of the directional brain–heart interplay, particularly indicating the following findings during prolonged baroreflex elicitation: (i) strong sympatho-vagal changes significantly increase the magnitude of the brain–heart directional coupling following inverse correlation dynamics for sympatho-vagal changes (i.e., the higher the brain activity, the lower the sympatho-vagal tone) mainly in the fronto-parietal regions; (ii) afferent vagal activity to the brain follows an inverse correlation dynamics mainly in the fronto-parietal regions, whereas efferent vagal activity from the brain follows direct correlation dynamics mainly in the ipsilateral frontal, prefrontal, and midline cortices; (iii) preferred brain oscillatory dynamics for the afferent autonomic outflow tend to occur within the δ and γ bands, whereas efferent autonomic control tends to occur through cortical oscillations in the θ , α , and β bands; (iv) from-brain-to-heart changes appear first (about 30 s), followed by changes in the coupling from-heart-to-brain with an approximate 30 s delay (60 s); and (v) lateralisation mechanisms occur throughout the systems information exchange in the θ band involving sympatho-vagal dynamics.

ELECTRONIC SUPPLEMENTARY MATERIAL

The online version of this article (<https://doi.org/10.1007/s10439-019-02251-y>) contains supplementary material, which is available to authorized users.

REFERENCES

- ¹Al-Nashash, H., Y. Al-Assaf, J. Paul, and N. Thakor. EEG signal modeling using adaptive markov process amplitude. *IEEE Trans. Biomed. Eng.* 51:744–751, 2004.
- ²Bashan, A., R. P. Bartsch, J. W. Kantelhardt, S. Havlin, and P. C. Ivanov. Network physiology reveals relations between network topology and physiological function. *Nat. Commun.* 3:702, 2012.
- ³Beissner, F., K. Meissner, K.-J. Bär, and V. Napadow. The autonomic brain: an activation likelihood estimation meta-analysis for central processing of autonomic function. *J. Neurosci.* 33:10503–10511, 2013.
- ⁴Benarroch, E. E. Central Autonomic Control. In: *Primer on the Autonomic Nervous System* (Third Edition), 2012, pp. 9–12.
- ⁵Brennan, M., M. Palaniswami, and P. Kamen. Poincare plot interpretation using a physiological model of hrv based on a network of oscillators. *Am. J. Physiol. Heart Circ. Physiol.* 283:H1873–H1886, 2002.
- ⁶Catrambone, V., A. Greco, M. Nardelli, S. Ghiasi, N. Vanello, E. P. Scilingo, and G. Valenza. A new modelling framework to study time-varying directional brain–heart interactions: preliminary evaluations and perspectives. In: *2018 40th Annual International Conference of the IEEE Engineering in Medicine and Biology Society*, pp. 4611–4614, IEEE, 2018.
- ⁷Chang, P. F., L. Arendt-Nielsen, and A. C. Chen. Dynamic changes and spatial correlation of eeg activities during cold pressor test in man. *Brain Res. Bull.* 57:667–675, 2002.
- ⁸Cui, J., T. E. Wilson, and C. G. Crandall. Baroreflex modulation of muscle sympathetic nerve activity during cold pressor test in humans. *Am. J. Phys.* 282:H1717–H1723, 2002.
- ⁹Dorrance, A. M. and G. Fink. Effects of stroke on the autonomic nervous system. *Compr. Physiol.* 5:1241–1263, 2015.
- ¹⁰Esler, M. D. Mental stress, panic disorder and the heart. *Stress and Health* 14:237–243, 1998.
- ¹¹Faes, L., D. Marinazzo, F. Jurysta, and G. Nollo. Linear and non-linear brain–heart and brain–brain interactions during sleep. *Physiological measurement* 36:683, 2015.
- ¹²Hering, D., K. Lachowska, and M. Schlaich. Role of the sympathetic nervous system in stress-mediated cardiovascular disease. *Current hypertension reports* 17:80, 2015.
- ¹³Lin, A., K. K. Liu, R. P. Bartsch, and P. C. Ivanov. Delay-correlation landscape reveals characteristic time delays of brain rhythms and heart interactions. *Phil. Trans. R. Soc. A* 374:20150182, 2016.
- ¹⁴Lovullo, W. The cold pressor test and autonomic function: a review and integration. *Psychophysiology* 12:268–282, 1975.
- ¹⁵Orini, M., R. Bailón, L. T. Mainardi, P. Laguna, and P. Flandrin. Characterization of dynamic interactions between cardiovascular signals by time-frequency coherence. *IEEE Trans. on Biom. Eng.* 59:663–673, 2012.
- ¹⁶Peng, R.-C., W.-R. Yan, X.-L. Zhou, N.-L. Zhang, W.-H. Lin, and Y.-T. Zhang. Time-frequency analysis of heart rate variability during the cold pressor test using a time-varying autoregressive model. *Physiological measurement* 36:441, 2015.
- ¹⁷Pola, S., A. Macerata, M. Emdin, and C. Marchesi. Estimation of the power spectral density in nonstationary cardiovascular time series: assessing the role of the time-frequency representations (tfr). *IEEE Transactions on Biomedical Engineering* 43:46, 1996.
- ¹⁸Pyner, S. The paraventricular nucleus and heart failure. *Experimental physiology* 99:332–339, 2014.
- ¹⁹Reshef, D. N., Y. A. Reshef, H. K. Finucane, S. R. Grossman, G. McVean, P. J. Turnbaugh, E. S. Lander, M. Mitzenmacher, and P. C. Sabeti. Detecting novel associations in large data sets. *Science* 334:1518–1524, 2011.
- ²⁰Schulz, S., M. Bolz, K.-J. Bär, and A. Voss. Central-and autonomic nervous system coupling in schizophrenia. *Phil. Trans. R. Soc. A* 374:20150178, 2016.
- ²¹Schwabe, L., L. Haddad, and H. Schachinger. Hpa axis activation by a socially evaluated cold-pressor test. *Psychoneuroendocrinology* 33:890–895, 2008.
- ²²Stankovski, T., T. Pereira, P. V. McClintock, and A. Stefanovska. Coupling functions: universal insights into dynamical interaction mechanisms. *Reviews of Modern Physics* 89:045001, 2017.
- ²³Stankovski, T., S. Petkoski, J. Raeder, A. F. Smith, P. V. McClintock, and A. Stefanovska. Alterations in the coupling functions between cortical and cardio-respiratory oscillations due to anaesthesia with propofol and sevoflurane. *Phil. Trans. R. Soc. A* 374:20150186, 2016.

- ²⁴Stokes, P. A. and P. L. Purdon. A study of problems encountered in granger causality analysis from a neuroscience perspective. *Proceedings of the National Academy of Sciences* 114:E7063–E7072, 2017.
- ²⁵Taggart, P., H. Critchley, and P. Lambiase. Heart–brain interactions in cardiac arrhythmia. *Heart* 97:698–708, 2011.
- ²⁶Tahsili-Fahadan, P. and R. G. Geocadin. Heart–brain axis: effects of neurologic injury on cardiovascular function. *Circulation research* 120:559–572, 2017.
- ²⁷Thayer, J. F., F. Åhs, M. Fredrikson, J. J. Sollers, and T. D. Wager. A meta-analysis of heart rate variability and neuroimaging studies: implications for heart rate variability as a marker of stress and health. *Neuroscience & Biobehavioral Reviews* 36:747–756, 2012.
- ²⁸Valenza, G., A. Duggento, L. Passamonti, S. Diciotti, C. Tessa, R. Barbieri, and N. Toschi. Resting-state brain correlates of instantaneous autonomic outflow. In: *Proc. of IEEE-EMBC*, pp. 3325–3328. 2017.
- ²⁹Valenza, G., A. Duggento, L. Passamonti, S. Diciotti, C. Tessa, N. Toschi, and R. Barbieri. Resting-state brain correlates of cardiovascular complexity. In: *2017 39th Annual International Conference of the IEEE Engineering in Medicine and Biology Society*, pp. 3317–3320, IEEE2017.
- ³⁰Valenza, G., A. Greco, C. Gentili, A. Lanata, L. Sebastiani, D. Menicucci, A. Gemignani, and E. Scilingo. Combining electroencephalographic activity and instantaneous heart rate for assessing brain–heart dynamics during visual emotional elicitation in healthy subjects. *Phil. Trans. R. Soc. A* 374:20150176, 2016.
- ³¹Valenza, G., N. Toschi, and R. Barbieri. Uncovering brain–heart information through advanced signal and image processing. *Phil. Trans. R. Soc. A* 374, 2016.